OPTION OF METHOD FOR ELECTRON BUNCH PHASE DISTRIBUTION MONITORING

A.Tron, I.Merinov, V.Smirnov,
MEPhI, Kashirskoe sh. 31, 115409 Moscow, Russia

Abstract

Methods for longitudinal bunch charge distribution monitoring can be divided onto two groups: the usings of coherent or incoherent radiation of the bunch electrons. The former can be used for estimation of the rms bunch length, and the latter - for the bunch charge distribution measurements. Methods of the bunch distribution monitoring with subpicosecond resolution based on use of secondary electrons, transition, Cherenkov or bremsstrahlung radiation are considered.

1 INTRODUCTION

Increasing interest in short electron bunches for different applications such as a linear collider, FEL, plasma or laser wakefield accelerators demands further development and creation of bunch length (BL) or bunch phase distribution (BPD) monitoring systems with subpicosecond and far better resolution.

All known methods for these measurements can be divided onto two groups: the usings of a coherent or incoherent radiation of the bunch electrons, i.e. the radiation on the wave lengths compared with the bunch length or considerably less than the BL.

It is known the former can be adopted for estimations of the rms BL [1,2,3,4,5,6]. The latter is for measuring the BPD without any model approach of the bunch distribution, and the beam instrumentation from this group form the metrological background for the BL or BPD monitoring. As to the tools of the first group they have to be simple and serve for fast operating control of the BL changes during the linac tuning. The instrumentation from both groups could complement to each other to obtain the complete monitoring system for a specific machine.

The principle of the BPD monitoring is based on the temporal analysis of the incoherent radiation including transition, Cherenkov, bramsstrahlung radiation and also secondary electron one.

The use of incoherent radiation, for example, on a scheme: Cherenkov radiator plus a streak camera [7,8,9], is mainly limited due to the longitudinal chromatic aberration of the camera gap (photocathode - mesh distance) caused by initial velocity spread of hpotoelectrons. To minimize this aberration in several tens times it was proposed [10] instead of a plane-parallel geometry of the gap to use emitter with a small radius of its surface.

The promising method for the BPD monitoring is the secondary electron one [10,11] allowing us to create the selfcalibrating monitor with resolution in the fs-range. This technique is simpler significantly than a streak camera because its rf-feed is taken from appropriate system of a linac. The rf-feed is locked in phase with the bunches, and in the case the time jitter (trigger jitter [12]) can be negligible.

2 SECONDARY ELECTRON MONITOR

One of scheme of secondary electron monitor for BPD measurements is shown in Fig.1.

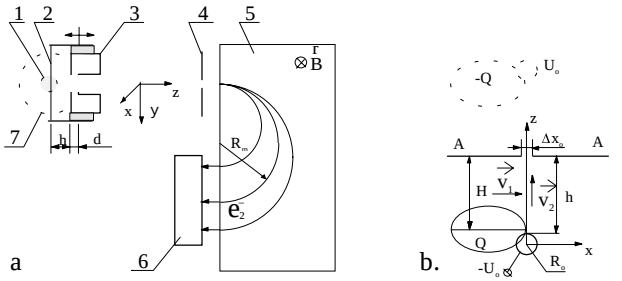

Figure 1: Layout of BPD monitor (a) and geometry of its primary converter (b).

Here BPD of a primary beam (1) in a result of the beam interaction with a wire emitter (2) being under negative potential (U_0) is isohronously transferred into the same distribution of secondary electrons which, then, is coherently transformed into transverse one in the plane of multichannel collector (6) through rf-modulation in the gap of toroidal resonator (3) and magnet (5) allowing direct presentation the BPD on a low frequency display. Taking into account that the beam diameter is rather small (of 1...2 mm), and the smaller h-distance the less transit time spread, the emitter was placed from the resonator at the small fixed distance h = 5 mm, and this monitor unit is moved in the beam for a time of measurement only.

The monitor phase resolution is mainly defined by the transit time spread of the electrons on the h-distance from the emitter with the R_0-radius to the conducting wall (A-A) of the resonator (3), the shutter phase resolution and additional phase dilution due to the beam space charge effect, considered in [13]. Restrictions on the limiting resolution of the shutter, as a rule, lay lower than it can be for the transit time spread, and we shall consider the latter more in detail.

0-7803-4376-X/98/$10.00 © 1998 IEEE

3 TRANSIT TIME SPREAD

Omitting the space charge effect the estimation of the transit time spread of the electrons in the accelerating gap can be done through the chromatic aberration of the gap and the aberration of diaphragm installed in its exit plane.

The chromatic aberration of the h-distance gap (being under the U_0-accelerating voltage) caused by initial electron kinetic energy spread, for example, from W_1 to W_2 can be determined from the expression

$$\Delta t = \frac{h}{c}\sqrt{\frac{W_0}{2U_0}}\left(\frac{2}{E_m/E_0}\frac{\sqrt{W_2}-\sqrt{W_1}}{\sqrt{U_0}} + \frac{W_2 - W_1}{2U_0}\right), \qquad (1)$$

where U_0 - in an electron energy units(eV), c is the speed of light, W_0 is the electron rest energy, E_m/E_0 is the retio of the maximum electric field strength on the emitter surface to the strength in the case of the uniform field, i.e., when the plane-parallel geometry of the gap is used.

Denoting $h/R_0 \equiv m$ the E_m/E_0-ratio is given by

$$E_m/E_0 = \sqrt{(m+1)^2-1}\Big/\ln\left(m+1+\sqrt{(m+1)^2-1}\right)$$

values of which as a function of m is represented in Fig.2.

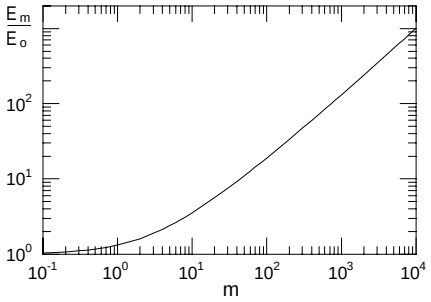

Figure 2: Maximum electric field strength on the emitter surface vs. the ration $m = h/R_o$.

Taking $m = 10^3$ one can increase the electric strength E_m by a factor of 10^2 and, as a consequence, minimize the longitudinal chromatic aberration significantly, that is show in Fig.3.

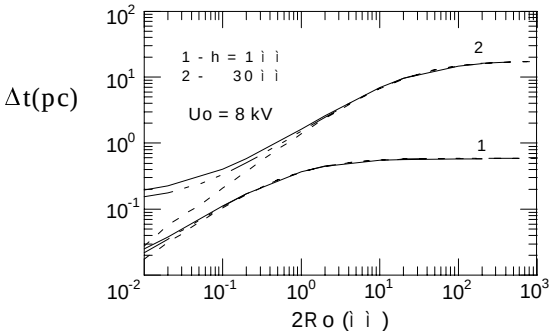

Figure 3: Longitudinal chromatic aberration of the gap vs. the emitter diameter for different distances h at $U_o = 8$ kV.

The solid lines in Fig.3 are the dependencies taken from [10], the dotted lines represent the calculation results on the formula (1), but the dotted line coming from the upper curve to the bottom one is obtained without the second term in the circular bracket of the formula (1). One can see that with decreasing R_o and h the longitudinal chromatic aberration of the gap can reach several tens fs.

It should be noted that with decreasing of h we will have to decrease, for example, the radius of the circular hole in the exit plane of the gap or increase the h-distance at the same output diaphragm so that the perturbation effect of the electric field, caused by this diaphragm, would be negligible.

Universal dependence of the transit time spread caused by the diaphragm with infinitesimal thickness in the case of plane-parallel gap vs. the ratio of the h-distance to the exit hole radius is represented in Fig.4, where $t_o = (2h/c)(W_o/2U_o)^{1/2}$ is the transit time in the gap without the hole. Magnitude of $\bullet t_D$ is defined as the FWHM of the transit time distribution of the electrons started with the 1eV energy perpendicular to the emitter surface and with uniform density of escaping.

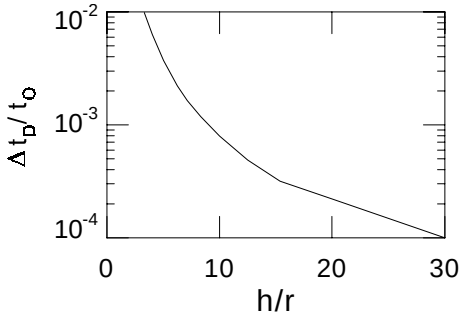

Figure 4: Transit time spread of electrons in the plane-parallel gap vs. its h-distance in units of the hole radius.

As an example, consider the gap of 1 mm with the 4 kV accelerating voltage, then the transit time of t_o will be 53 ps, and to get the spread not more than 0.05 ps the hole radius of about 0.1 mm has to be taken. Another words, in some cases the account of the diaphragm aberration can decrease the device capacity significantly.

4 RF GAP

To minimize the space charge effect of the relativistic electron beam with the bunch population of $5 \cdot 10^{10}$ and more one can place the rf-gap of the monitor resonator in the beam [13] so that the directions of moving both the primary beam and the secondary one are coincided in the accelerating and rf-modulating gaps. It is permissible, for example, when the frequency of the bunches is rather low. In the case the rf-gap in the form of two plane-parallel strips from thin foil is placed in the beam so that their planes are perpendicular to the beam axis, and the inductance part of the resonator is outside of the beam pipe. As an example, in Fig.5 is shown the phase resolution of the 1 mm rf-gap with 3 kV amplitude of rf-voltage on the 3 GHz frequency vs. input secondary

electron phase for two cases: when initial electron energy is 4 keV (2) and when the electron is accelerated till this energy in the uniform static field in the rf-gap (1). Hence, at the same electrical and geometrical parameters of the monitor the second case is far more effective.

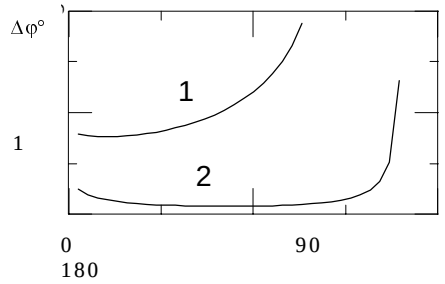

Figure 5: Phase resolution of the 1 mm rf-gap.

5 DELTA-RAYS

One of the way of the BPD monitoring with resolution in the fs-range is the use of the delta-electrons [11]. In Fig.6 the time distribution of the delta-electrons with energies of 10 and 50 keV scattered by the 10 MeV electrons in the carbon fibre of the 8 μm diameter is shown. Probability of escaping of the delta-electron captured by the 1 mm diameter collimator hole, spaced from the target on 5 mm so that the axes of the primary and secondary beams are perpendicular, is about $2 \cdot 10^{-8}$ per an electron of the primary beam with uniform current density distribution within its radius of 1 mm and at analysis of the delta-electrons within energy range of (10±0.05) keV. At the target from the tungsten the probability will be by an order of magnitude greater.

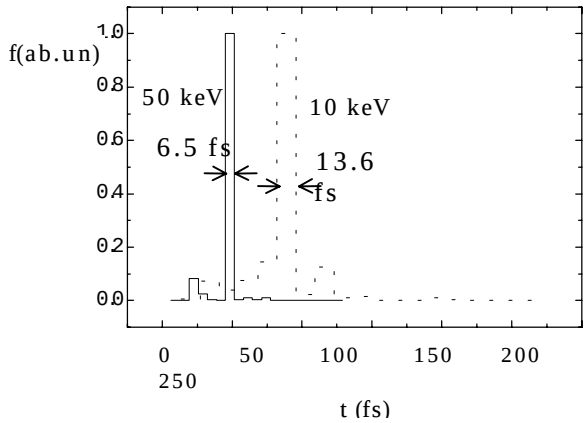

Figure 6: Time distribution of the delta-electrons with energy 10 and 50 keV scattered by the 10 MeV electrons in the carbon fibre of the 8 μm diameter.

6 X-RAYS

At present the x-ray streak camera resolution is limited by 1 ps [14] due to the chromatic aberration of the gap. Improving this resolution by the way mentioned above we have to estimate the efficiency of the x-ray use in our case. Dependence of the x-ray yield per an electron scattered in the tungsten wire of the 0.1 mm diameter (at the same geometry similar to the case of the delta-electron use) vs. the electron energy is shown in Fig.7 where the yield has been defined for the x-ray energy within the range of 1-10 keV. At the calculation the cross sections from [15,16] have been used.

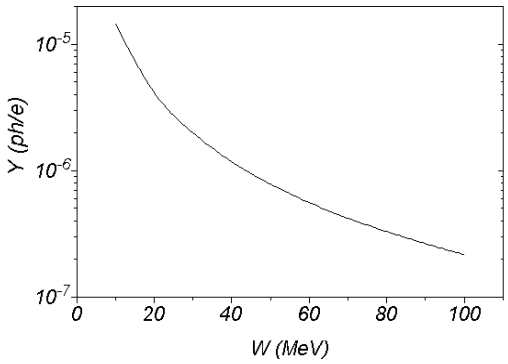

Figure 7: X-rays yield per scattered electron vs. the electron energy.

7 CONCLUSIONS

As it was shown there exist several methods for the BPD measurements with high resolution, and its option depends on the terms in a specific machine .

8 ACKNOWLEDGMENTS

The researches were supported by the Russian Fund for Fundamental Investigations.

REFERENCES

[1] R.H.Miller, et al., IEEE Trans.Nucl.Sci., NS-12, 804 (1965).
[2] E.Babenko, et al., SLAC-PUB-6203 (1993).
[3] A.V.Aleksandrov, et al., AIP Conf. Proc.333, 452 (1994).
[4] T.Nakazato, et al., Proc. of the LINAC94 Conf., 890 (1994).
[5] H.Linh, et al., SLAC-PUB-95-6958 (1995).
[6] D.X.Wang, Proc. of the LINAC96 Conf., 303 (1996).
[7] Y.C.Sheppard, et al., IEEE Trans.Nucl.Sci., NS-32, 2006 (1985).
[8] M.Uesaka, et al., Proc. of the LINAC94 Conf., 804 (1994).
[9] E.K.Zavoysky, S.D.Funchenko, Dok.Akad.Nauk, 226, 1062 (1976).
[10] A.Tron, et al., Proc. of the LINAC96 Conf., 514 (1996).
[11] A.Tron, et al., Proc. of the LINAC96 Conf., 517 (1996).
[12] Guide to Streak Cameras. 1994 Hamamatsu Photonics K.K.
[13] A.Tron, I.Merinov, "Space Charge Effect in Secondary Electron Monitors", this Conf.
[14] R.Shepherd, et al., Rev.Sci.Instrum. 66 (1), 719 (1995).
[15] H.W.Koch, et al., Rew.Mod.Phys., 31 (4), 920 (1959).
[16] S.M.Seltzer, et al., NIM, Phys.Res., B12, 95 (1985).